

Changing fluorescence in a streaming barium plasma due to an axial magnetic field

Keith D. Bonin and Thomas G. Mason

Department of Physics, Princeton University, Princeton, New Jersey 08544

(Received 1 October 1990)

The present investigations consider the case of a low-density laser-produced plasma expanding into a vacuum in the presence of an axial magnetic field. The time-integrated line intensities of neutral and singly ionized barium have been measured for magnetic fields up to 300 G. These measurements reveal three prominent changes in the intensities of individual lines as a function of increasing magnetic field: extinction, growth, and severe attenuation followed by enhancement. Measurements support a model that predicts the quenching of higher-lying transitions and the enhancement of lower-lying transitions for increasing magnetic fields.

INTRODUCTION

The effect of a magnetic field on an expanding laser-produced plasma has been the subject of many theoretical and experimental investigations.¹⁻⁵ An understanding of the effects of a magnetic field on a streaming plasma is useful in many areas of laboratory and astrophysical plasma physics. Important examples include the study of sunspots, supernova, and geomagnetic effects in the atmosphere.

This paper reports detailed quantitative measurements of the changing fluorescence of a low-density, streaming barium plasma in an axial magnetic field. An example of the dramatic changes in the fluorescence that can occur when a magnetic field is applied to a flowing plasma is given in Fig. 1. Changes in the fluorescence of low-density laser and discharge plasmas in applied magnetic fields have been previously reported.⁴⁻⁸ Some reports indicate only radiative enhancement due to the magnetic field, while others measure an initial dip in the plasma luminosity for low magnetic fields.⁸ Enhancing the luminosity of low-density discharge plasmas by applying a magnetic field has possible applications in the lamp industry. To date, changes in lamp discharge luminosities with magnetic field are poorly understood.⁷

A detailed quantitative investigation of the line radiation emitted by a streaming plasma in a low magnetic field has not been previously reported. Such an investigation provides evidence which must be explained by the fundamental mechanisms which produce the changes in fluorescence of the plasma in the magnetic field. These mechanisms might explain the previously reported attenuation and enhancements in other low-density plasmas.

The plasma was highly reproducible throughout all the experiments, and simple diagnostics were used to measure the important characteristics of the plasma 10 cm downstream from the source: electron density and temperature; ground-state neutral atom density and timing; and ion density and timing. Barium was chosen to be the target metal because its principal neutral and ion lines

conveniently occur in the visible region of the optical spectrum. A charge-coupled-device (CCD) camera, a Langmuir probe, a tunable diode laser, and a line fluorescence detection system were used to investigate the flowing plasma-field interaction.

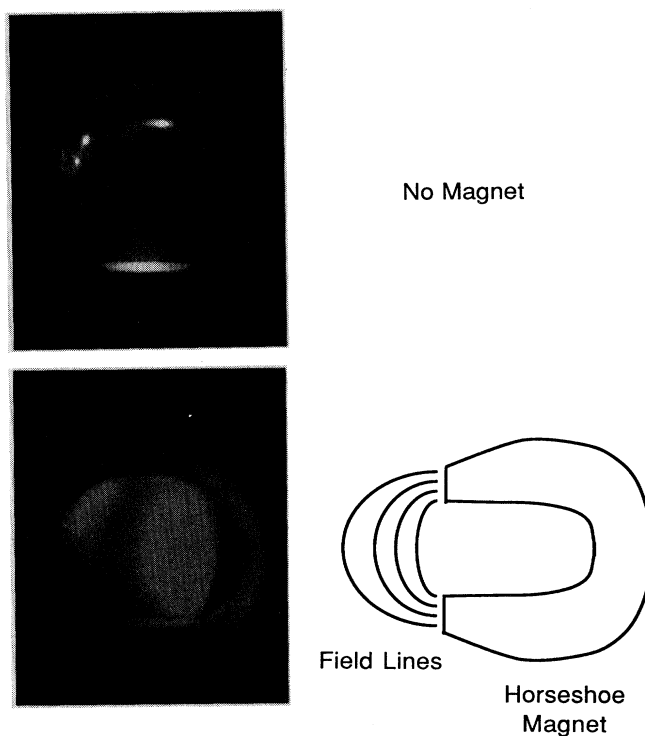


FIG. 1. Images taken with a CCD camera reveal the spatial variations of fluorescence in the central region of the chamber when (a) no magnetic field was applied and (b) when a 1-kG horseshoe magnet was placed next to the chamber as indicated. The laser-produced plasma flows up in these images. The viewing region is 10 cm from the barium target. The spatial distribution of the enhanced fluorescence shows that the radiation is highly localized.

EXPERIMENT

The streaming plasma was generated by irradiating a barium target with unfocused light at a wavelength $\lambda = 532$ nm from a doubled Nd:YAG (yttrium aluminum garnet) laser operating at 10 Hz. The barium target was a disk 2.5 cm in diameter and 1.5 cm thick. Each laser pulse had a temporal pulsewidth of 10 ns, an energy of 380 mJ, and an area of 0.2 cm^2 . The vacuum chamber consisted of a six-way glass cross mounted to an aluminum stand (Fig. 2). A grounded aluminum tube was inserted into the arm of the cross containing the target. The barium target, which was also electrically grounded, could be rotated in the vacuum using a rotary feed-through located at the bottom arm. An aluminum wedge at the top arm held a pyrex window at Brewster's angle to provide maximum transmission of laser power. A turbomolecular pump maintained the vacuum chamber at a typical operating pressure of $\approx 2 \times 10^{-6}$ torr, as measured by a nude ion gauge.

Magnetic fields from 0 to 300 G were generated using

water-cooled Helmholtz coils. The field was constant to better than 1% over the length of the chamber viewing region along the magnetic-field axis. A high-current power supply provided the current to drive the coils. A digital voltmeter measured the voltage drop across a 0.01Ω resistor and thus monitored the current to the coils. The voltage-field characteristic of the Helmholtz coils was determined using a commercial Hall probe.

Plasma radiation was detected by focusing light from the central viewing region of the six-way cross onto the entrance slit of a 0.5 m scanning monochromator. The focusing lens, located about 15 cm from the central region, collected all the light exiting one of the side viewing arms. The circular viewing arm was 5 cm in diameter and was located about 10 cm downstream of the plasma production region at the target. The monochromator slits were $75 \mu\text{m}$ wide to improve light collection at a cost of resolution, which was limited to about 1.5 \AA . The signal from a photomultiplier tube (PMT) mounted at the exit slit of the monochromator was sent to a strip-chart recorder or to a gated integrator. The PMT bias was ad-

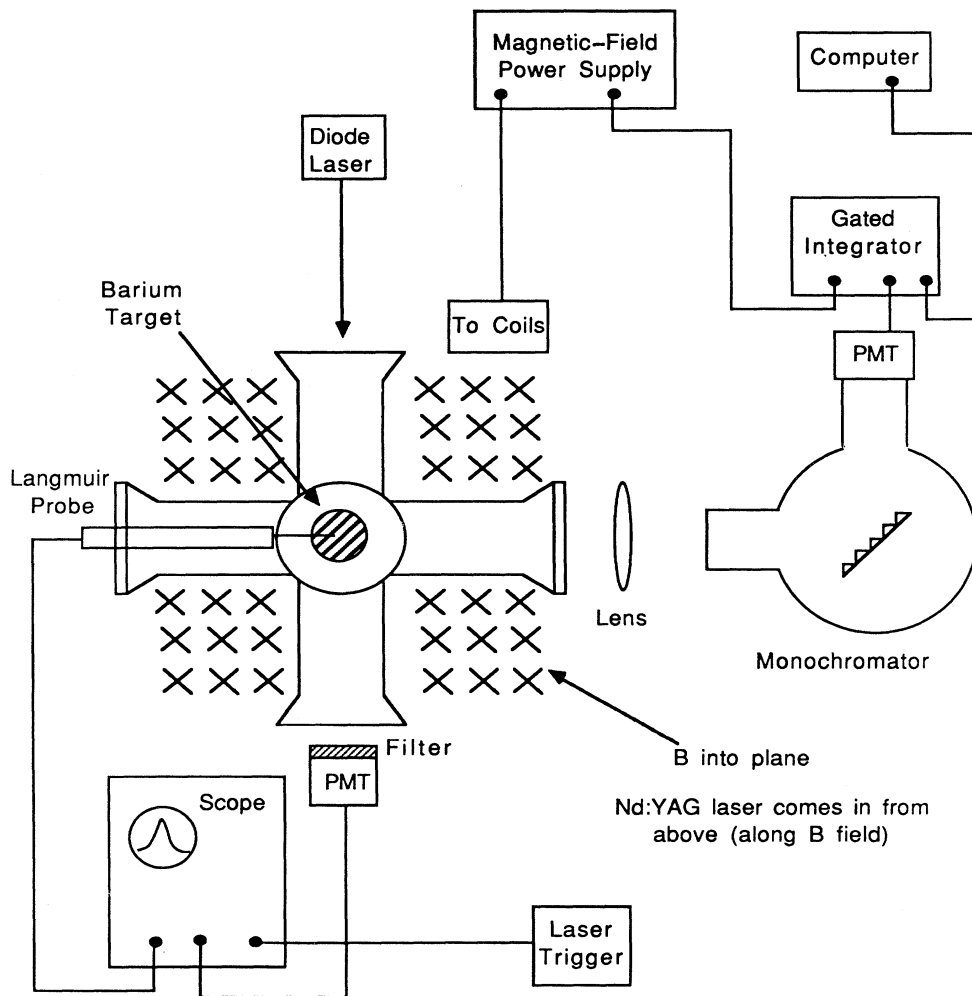


FIG. 2. This diagram shows the experimental setup as viewed from the top. A pair of Helmholtz coils that are not shown produced a magnetic field oriented perpendicular to the plane of the paper.

justed according to the strength of the particular line being investigated. However, for a scan over a large spectral range, the PMT bias was held fixed and its output signal was sent to a strip-chart recorder. The photomultiplier tube was biased between 400 and 1000 V and was magnetically shielded to ensure its proper operation at all accessible fields. The effectiveness of the magnetic shielding was verified to better than 1% by comparing the response of the PMT with a mercury line produced by a room light in zero applied field with its response in maximum applied field.

Photomultiplier signals were temporally integrated by a fast gated integrator. Both the integrated signal and the magnetic-field voltage were sent to an analog-to-digital converter (ADC). The ADC outputs were recorded by a microcomputer. Gate widths ranging from 5 to 100 μ s were used. The delay and width of the integration gate were adjusted so that the gate overlapped the entire fluorescence peak of the specified line. The data for a typical line were taken by sweeping the magnetic field from 0 to 300 G and recording the integrated fluorescence and magnetic-field voltages. The intensity-field data for each line consisted of 1000 points and took roughly 2 min to collect.

Electron density and temperature were measured by inserting a Langmuir probe into the vacuum chamber close to the center of the viewing region. The exposed probe tip was a copper wire of diameter 100 μ m and length 1.9 cm. The probe was not present when the fluorescence measurements were performed. It was oriented normal to the streaming velocity and the magnetic field.

The use of a Langmuir probe as a diagnostic in a flowing plasma at zero magnetic field has been carefully investigated.⁹ From these studies it is clear that the signal from the Langmuir probe in a flowing plasma can be properly interpreted provided several conditions are satisfied.

(1) The potential difference ($V_b - V_0$), where V_b is the probe bias and V_0 is the plasma potential, must be kept small enough so that the net electrostatic energy does not exceed the mean kinetic energy of the ions in the flow direction, i.e., $e|V_b - V_0| \ll \frac{1}{2}M_i U^2$, where the quantity M_i is the ion mass and U represents the mean longitudinal or flow speed of the ions.

(2) The electron thermal velocity c_e must greatly exceed the mean speed of the ions in the flow direction, i.e., $c_e \gg U$.

(3) The collisional mean free path λ_c must be large compared with the probe radius r_p and the electron Debye length λ_D , i.e., $\lambda_c \gg r_p$, $\lambda_c \gg \lambda_D$. All of these conditions were met by the flowing barium plasma discussed here. The Langmuir probe was connected to a gated integrator which sampled the signal at 4.6 μ s after the laser pulse using a 250-ns wide gate. The integrated signal and the bias voltage were recorded by the computer. The probe bias potential was swept from -25 to $+25$ V. A typical scan consisted of 500 data points.

A continuous-wave, tunable diode laser was used to determine the timing and density of the ground-state barium neutrals. These characteristics were measured by

considering the absorption of light resonant with the Ba $6s^2\ ^1S_0 \rightarrow 6s6p\ ^3P_1$ line at 7913 Å (see Fig. 3). The laser had a linewidth of less than 10 MHz and a beam area in the central region of about 0.5 cm². The absorption measurements were performed with an attenuated laser power of about 0.1 mW. The transmitted light passed through interference and neutral density filters and was then detected using a PMT.

In the final measurement, spatial variations in the fluorescence from the central region of the vacuum chamber were detected using a CCD camera. Images were stored on a computer using a framegrabber. Images of the total fluorescence at wavelengths greater than 5900 Å were taken at various magnetic-field strengths. This was accomplished by placing appropriate color glass filters in front of the camera lens. A 532-nm rejection filter and neutral density filters were also simultaneously used. These images were taken to record spatial variations in intensity that occurred in the viewing region under different magnetic-field conditions. Images of the central region were also recorded while a horseshoe magnet ($B_{\max} \lesssim 1$ kG) was held next to the chamber walls (see Fig. 1).

EXPERIMENTAL RESULTS

Visual observations of the plasma fluorescence using RG595 (Schott Glass) protective goggles (Fred Reed Optical) indicated the minimum in total luminosity above 6000 Å occurred for magnetic fields of approximately 75 G. The overall luminosity appeared at least several times greater for maximum applied field than for zero applied field.

Visual observations and camera images of the plasma intensity indicated spatial variations in plasma density within the central observation region of the chamber for a uniform magnetic field of 190 G. The fluorescence emanating from the region halfway between the wall and center of the chamber was more intense than the fluorescence emanating from the center of the chamber and near the walls. When an inhomogeneous magnetic field was applied to the viewing region, significant spatial variations in the fluorescence were also observed. The fluorescence emitted near the poles of the horseshoe magnet was greatly enhanced. A few centimeters away from the poles there was a dark region, and even farther away from the poles the fluorescence was bright again (see Fig. 1). The enhancement in the emitted fluorescence was dramatic and highly localized.

A demonstration of the extreme changes in the plasma spectrum is shown in Fig. 4. The monochromator was scanned over a large range of wavelengths for two different fields: Fig. 4(a) shows the spectrum from 4000 to 5200 Å at $B=0$ G; Fig. 4(b) shows the same spectrum at $B=190$ G. These plots are reliable tracings of strip-chart recordings. Absolute and, to a lesser extent, relative intensity information is difficult to deduce from these plots due to collection geometry factors, the variation in PMT quantum efficiency with wavelength, the variation of the grating efficiency with wavelength, and shot-to-

shot variations in plasma conditions. The intensity ratio of the fluorescence produced by the same line at two different magnetic-field strengths is the most reliable and useful quantitative information that can be deduced from these plots. For reference, the peak intensity of the 4935-Å line was 14 times larger for $B=190$ G than for $B=0$ G fields. The intensity of this line was 70 times larger than its zero-field value at $B=300$ G. Overall, these plots emphasize the dramatic nature of the changes in the fluorescence due to the magnetic field.

Eight Ba lines and six Ba^+ lines were selected for study because of their noticeable intensity changes in the presence of the magnetic field. The observed lines can be categorized according to the shape of their fluorescent intensity (I) versus magnetic field (B) curves (see Fig. 5). Three qualitatively different intensity-field curves were observed: extinction—curves in which higher-lying ion and neutral transitions exhibited a sharp decrease in intensity with increasing magnetic field; growth—curves in which the low-lying ion lines show a large increase in intensity with increasing magnetic field; minima—curves in which low-lying neutral lines first decrease in intensity, reach a minimum, and then grow in intensity for larger

magnetic fields. A summary of the I - B curves for the 14 lines examined in the experiment is given in Table I. The table is sorted according to the dominant feature of the I - B curves. All of the I - B curves except two exhibit a minimum that is above the noise. The two exceptions are the I - B curves for the neutral 5160-Å line and the ion 4132-Å line; these have no resolvable minima due to noise.

Fives lines have the typical qualitative behavior of the rest, and the I - B characteristic curves for these lines are presented in Fig. 5. Each of these lines is identified in the last column of Table I. These five curves are representative samples of the qualitative features observed in the entire set I - B curves, although each line has its own particular features. The I - B characteristic curves were produced using a computer program to normalize the integrated intensity and calculate the magnetic field for all digitized data. At the highest field strength the absolute intensity of the 6143-Å ion line was about five times greater than that of the 5537-Å primary neutral line.

Oscilloscope photographs of the unintegrated fluorescence pulse indicated that the time difference between the arrival of the fluorescence peak and the laser trigger was

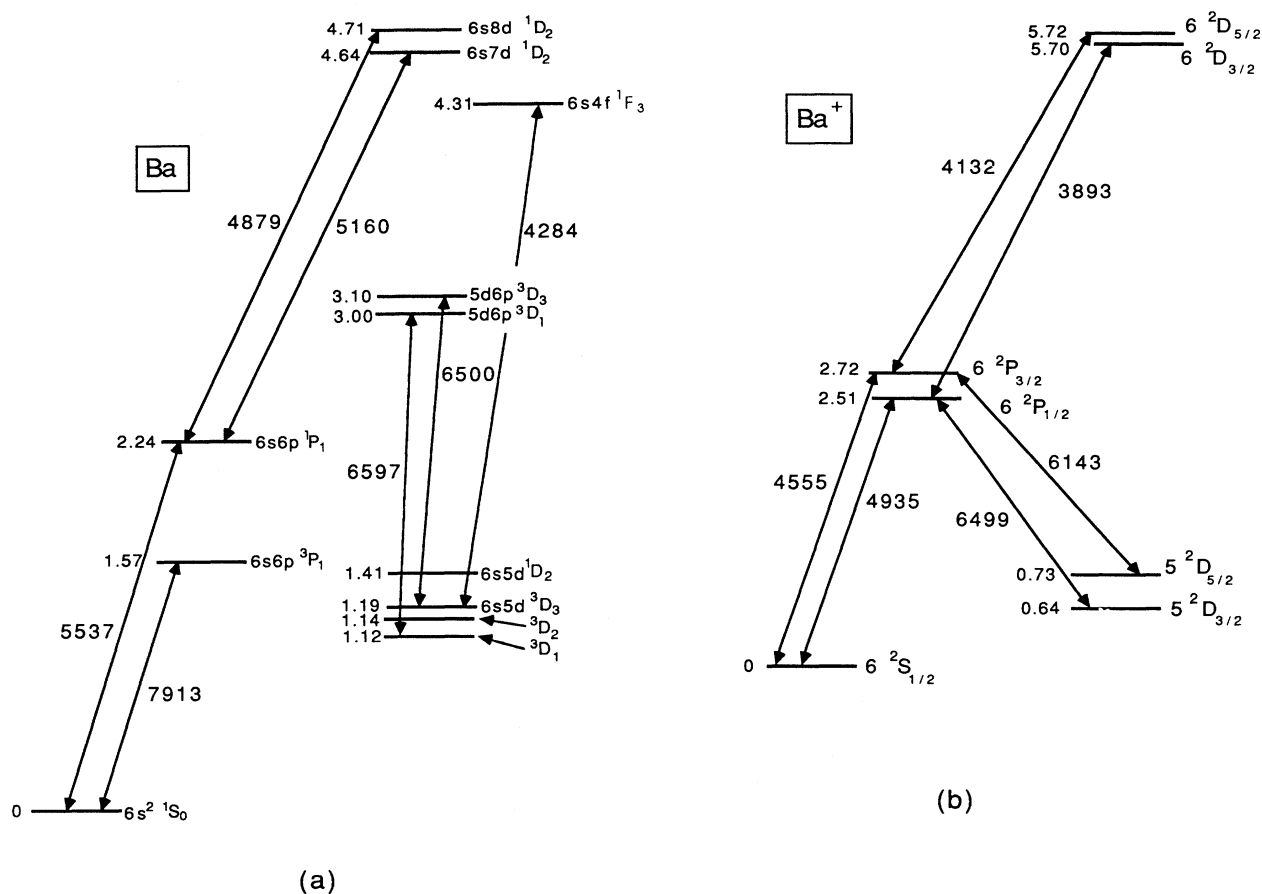


FIG. 3. Energy-level diagrams for (a) neutral barium and (b) singly ionized barium. Only those levels relevant to the data discussed in this paper are shown. The energies are given in eV and the wavelengths of the transitions are given in Å.

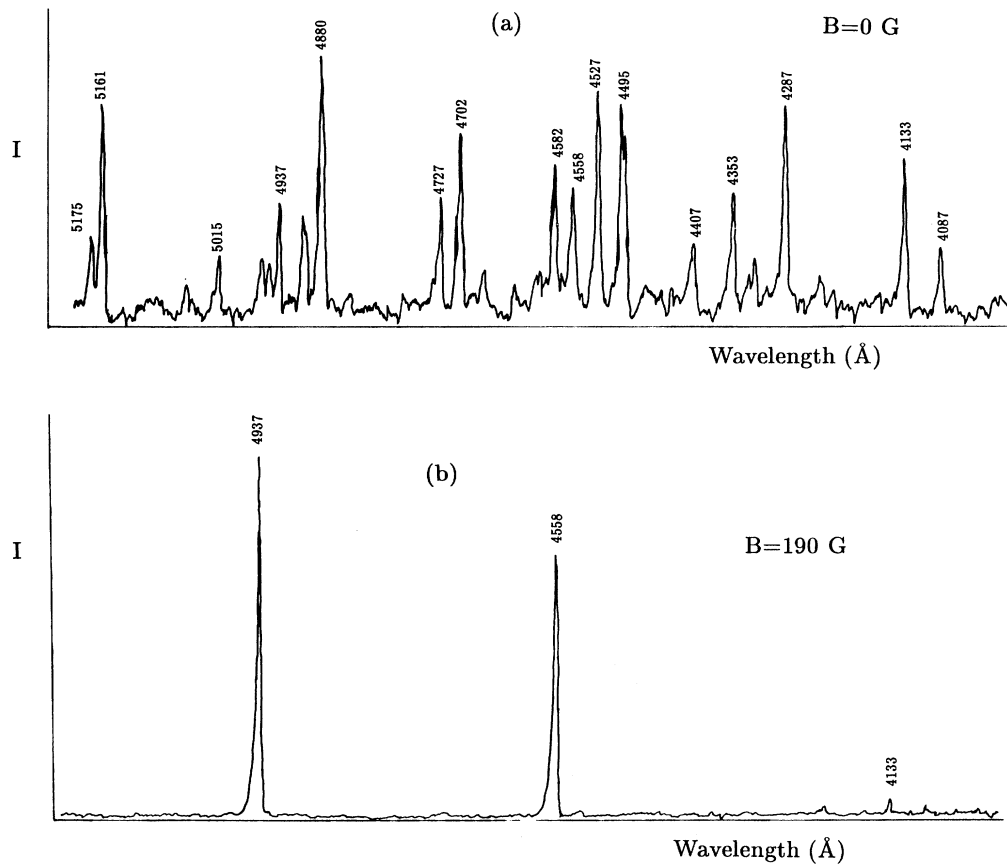


FIG. 4. Fluorescent intensities over a large spectral region: (a) scan from 4000 to 5200 Å with $B=0$ G, (b) scan from 4000 to 5200 Å with $B=190$ G. The low-lying Ba^+ lines clearly dominate the spectrum at high-field values, whereas the many high-lying ion and neutral lines that were present at $B=0$ G are entirely absent at $B=190$ G. The scale in (a) is five times more sensitive than that for (b). The 4935-Å Ba^+ line increased a factor of 14 when the field was raised to 190 G. The lines are labeled according to the measurements made from the strip-chart recordings and the discrepancy between these labels and the actual wavelengths of the lines is due to measurement error.

TABLE I. Summary of fluorescence versus magnetic-field data for Ba and Ba^+ .

I - B characteristic	Line (Å)	Source	Transition	E_u (eV) ^a	Figure
Minimum	7913.5	Ba	$6s6p\ ^3P_1 \rightarrow 6s^2\ ^1S_0$	1.57	
Deep minimum	5537.0	Ba	$6s6p\ ^1P_1 \rightarrow 6s^2\ ^1S_0$	2.24	5(a)
Deep minimum	6597.2	Ba	$5d6p\ ^3D_1 \rightarrow 5d6s\ ^3D_1$	3.00	
Deep minimum	6500.6	Ba	$5d6p\ ^3D_3 \rightarrow 5d6s\ ^3D_3$	3.10	5(b)
Minimum	6484.7	Ba	$5d6p\ ^1F_3 \rightarrow 5d6s\ ^1D_2$	3.33	
Large increase	6143.4	Ba^+	$6p\ ^2P_{3/2} \rightarrow 5d\ ^2D_{5/2}$	2.51	5(c)
	4935.5	Ba^+	$6p\ ^2P_{3/2} \rightarrow 6s\ ^2S_{1/2}$	2.51	
	6498.7	Ba^+	$6p\ ^2P_{1/2} \rightarrow 5d\ ^2D_{3/2}$	2.72	
	4555.3	Ba^+	$6p\ ^2P_{1/2} \rightarrow 6s\ ^2S_{1/2}$	2.72	
Extinction	4284.3	Ba	$6s4f\ ^1F_3 \rightarrow 6s5d\ ^1D_2$	4.31	
	5160.0	Ba	$6s7d\ ^1D_2 \rightarrow 6s6p\ ^1P_1$	4.64	
	4879.0	Ba	$6s8d\ ^1D_2 \rightarrow 6s6p\ ^1P_1$	4.78	5(d)
	3892.9	Ba^+	$6d\ ^2D_{3/2} \rightarrow 6p\ ^2P_{1/2}$	5.70	5(e)
	4131.8	Ba^+	$6d\ ^2D_{5/2} \rightarrow 6p\ ^2P_{3/2}$	5.72	

^aThe quantity E_u is the energy of the upper level of the fluorescent transition with respect to the ground state of its source, either neutral or ion. Note that the ionization potential of barium is $I_p=5.21$ eV.

about $9 \mu\text{s}$ for excited ions and $12 \mu\text{s}$ for excited neutrals at zero field [see Fig. 6(a)]. For ground-state neutrals the peak in the diode laser absorption signal occurred at roughly $23 \mu\text{s}$ for zero field. According to a time-of-flight analysis, the longitudinal streaming velocities of the vari-

ous components of the plasma at zero magnetic field were: $1 \times 10^6 \text{ cm/s}$ for excited Ba^+ ions, $8 \times 10^5 \text{ cm/s}$ for excited Ba, and $4 \times 10^5 \text{ cm/s}$ for ground-state Ba.

The rms thermal velocities of the different constituents are important because they determine the transverse tem-

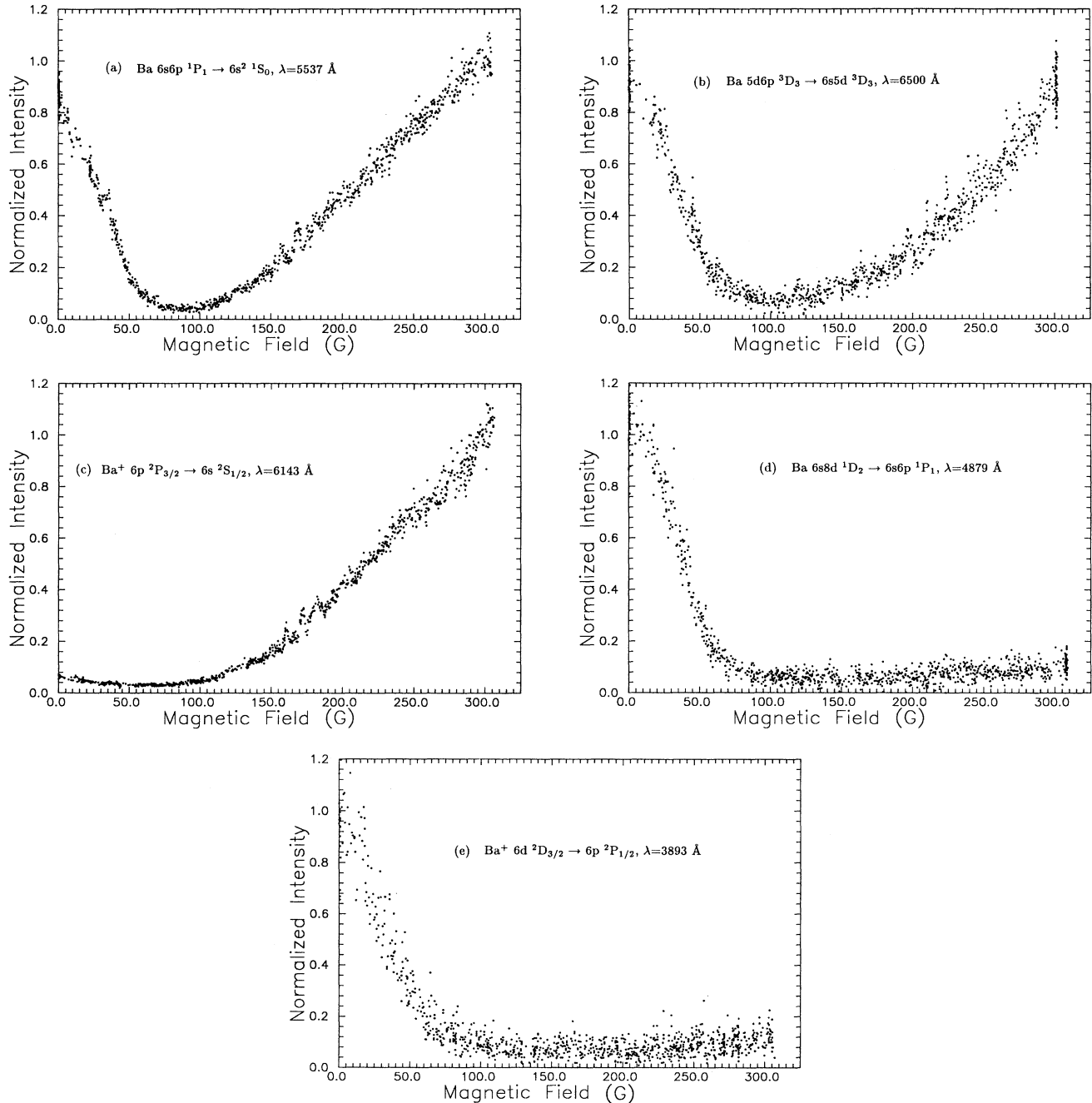


FIG. 5. Plots showing the fluorescent intensity of various ion and neutral barium lines 10 cm downstream from the laser-ablated source as a function of the axial magnetic-field strength. The different curves illustrate the three different types of behavior: (a) the $\text{Ba } 6s6p \ ^1P_1 \rightarrow 6s^2 \ ^1S_0$ line at 5537 \AA shows a large decrease in intensity to a minimum and a subsequent increase in fluorescence with increasing magnetic field, (b) the $\text{Ba } 5d6p \ ^3D_3 \rightarrow 5d6s \ ^3D_3$ line at 6500 \AA exhibits a curve similar to the previous line, (c) the $\text{Ba}^+ \ 6p \ ^2P_{3/2} \rightarrow 5d \ ^2D_{5/2}$ line at 6143 \AA shows a large increase in fluorescence with increasing magnetic field (note the small dip at low field values), (d) the $\text{Ba } 6s8d \ ^1D_2 \rightarrow 6s6p \ ^1P_1$ line at 4879 \AA shows extinction of a high-lying neutral line with increasing magnetic field, and (e) the $\text{Ba}^+ \ 6d \ ^2D_{3/2} \rightarrow 6p \ ^2P_{1/2}$ line at 3893 \AA shows the extinction of a high-lying ion line with increasing magnetic field.

peratures. These temperatures are related to the collision frequencies of the various possible scattering partners. The electron temperature T_e and number density n_e were determined from a measurement of the Langmuir probe current versus bias potential.^{9,10} From the probe measurements, the following values for these quantities at zero magnetic field were deduced: $T_e = 0.84 \pm 0.30$ eV and $n_e = (2.5 \pm 1.2) \times 10^{10}$ cm⁻³. From the relation between the temperature and the most probable velocity for a Maxwellian velocity distribution

$$v = \left(\frac{8kT_e}{\pi m_e} \right)^{1/2}, \quad (1)$$

the most probable transverse velocity of the electrons in the plasma is $v_{e\perp} = 6.1 \times 10^7$ cm/s. The quantity $k = 1.38 \times 10^{-16}$ erg/K is Boltzmann's constant. The

maximum transverse velocity of the neutral barium atoms in the central region can be estimated using geometry. The inner diameter of a chamber wall was 5.0 cm and the atoms traveled 10 cm from the source in 23 μ s (peak) which gives the value $v_{\perp\text{max}} = 8.7 \times 10^4$ cm/s. However, a measurement of the transmission of the diode laser light at 7913 Å versus wavelength indicates the atoms have a Doppler width of $\Delta\nu_D = 1$ GHz. This yields a more reliable value for the thermal velocity of the atoms:

$$v_{\perp} = \frac{\Delta\nu_D}{\nu} c = 8.0 \times 10^4 \text{ cm/s}, \quad (2)$$

where ν is the frequency of the diode laser and c is the speed of light. This latter value for v_{\perp} gives a neutral barium temperature of $T_{\text{atoms}} = 0.36$ eV at 23 μ s. The neutral barium ground-state number density 10 cm from

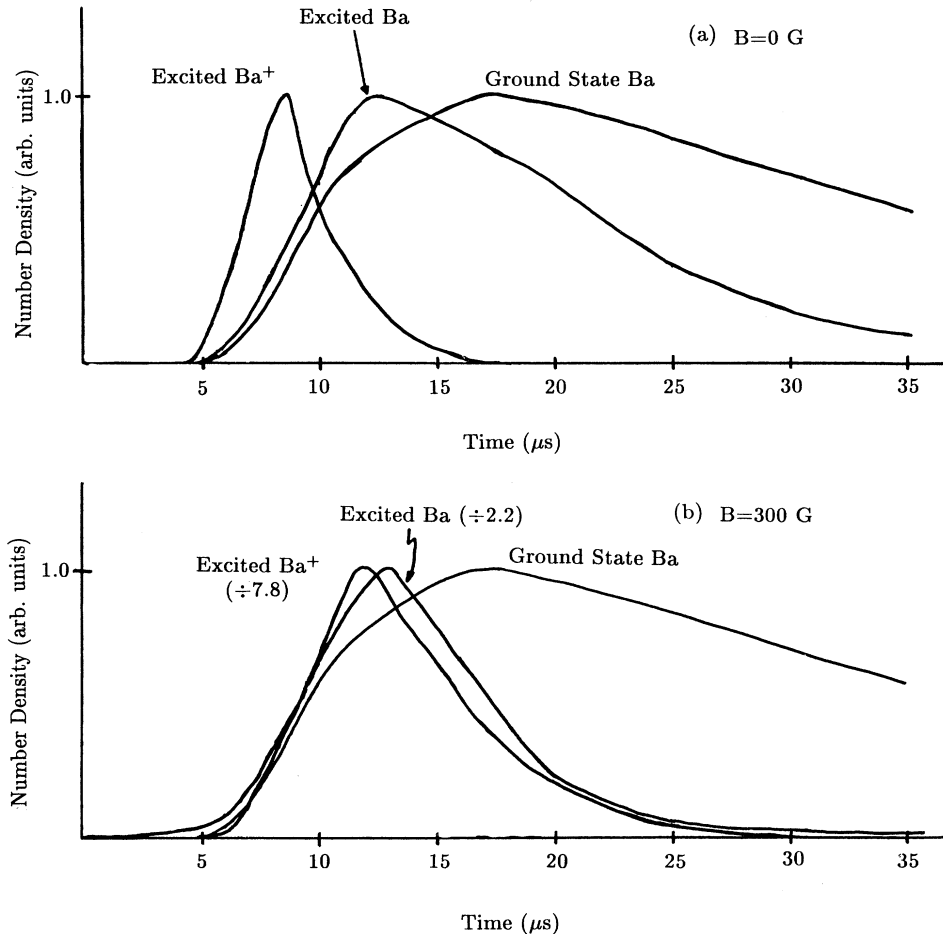


FIG. 6. A sketch of the timing of the different plasma species at zero magnetic field and at maximum magnetic field, reconstructed from oscilloscope photographs. The excited neutral and excited ion curves correspond to the fluorescence from the 6597-Å line and the 6143-Å line, respectively. The ground-state neutral timing was measured from the absorption of a diode laser tuned to the Ba 7913-Å line. (a) corresponds to the case where $B=0$ G and note that the peaks of all curves were arbitrarily scaled to unity. In (b), where $B=300$ G, the curve for each species is drawn with the correct magnitude relative to the corresponding curve in (a). The $B=300$ G curves for the excited neutral and excited ion lines have been scaled down by the factors indicated.

the source was $n_{\text{atoms}} = (3.0 \pm 0.5) \times 10^{11} \text{ cm}^{-3}$, as determined from the diode laser absorption measurements. This number was constant within experimental uncertainties as a function of magnetic-field strength. With a fractional ionization of about 10%, the plasma can be considered partially ionized.

Measurements of the electron density, temperature, and timing under application of the B field would be most helpful to the establishment of a particular model for the fluorescence results. However, from theoretical and experimental investigations of the use of a cylindrical Langmuir probe in nonzero magnetic field,^{11,12} it is clear that the interpretation of the resulting currents must be made with great care. The interpretation is difficult because a static electric field exists in the sheath surrounding a biased probe and this causes a reduction in the electrons in the sheath. Thus, the probe currents in magnetoplasmas are sensitive to collisional dynamics which makes the measurement difficult to understand. For strong fields, in which the probe radius r_p is larger than the Larmor radius a_L , $r_p \gtrsim a_L$, observed electron currents decreased relative to their zero-field values. Additionally, in strong fields the "knee" in the I_e - V_b curve became blurred.

Laframboise and Rubinstein¹¹ derived expressions for the electron current I_e versus bias potential V_b in the adiabatic limit ($a_L \gg L$, where L is the characteristic length scale for changes in the sheath potential around the probe), and they predicted the existence of a "negative resistance"

$$\frac{dI_e}{dV_b} < 0, \quad (3)$$

which has only been observed for probes oriented parallel to \mathbf{B} . In the present experiment, the following values for important plasma parameters were deduced from measurements at zero magnetic field: Debye length $\lambda_D = 44 \mu\text{m}$; probe radius $r_p = 50 \mu\text{m}$; $L \approx 1.5(eV_b/kT_e)^{1/2}$ in units of λ_D .

The delay and broadening of the ion arrival times in the central region of the chamber were confirmed by both the Langmuir probe ion current measurements and by the ion fluorescence measurements.

A number of the measurements reported above were repeated with the magnetic-field polarity reversed. There were no observable differences in the data for the two different magnetic-field polarities.

DISCUSSION

The enhanced fluorescence of the Ba^+ 4555-Å line seen by Jellison¹³ for a barium plasma flowing across a transverse magnetic field was explained by an $\mathbf{E} \times \mathbf{B}$ effect. According to his explanation, the plasma was polarized due to separation of the electrons and ions during plasma expansion. The resulting electric field, perpendicular to the magnetic field, produced an $\mathbf{E} \times \mathbf{B}$ motion that accelerated and heated the electrons. The final result was an increase in ionization and ion excitation which produced an increase in ion fluorescence. In contrast, the magnetic field in the present experiment was axial. Since

$|\mathbf{E} \times \mathbf{B}| = 0$, motion similar to the case of Jellison was absent in these experiments. For this reason polarization effects are ignored in the model discussed below.

The changes in the neutral and ionic fluorescence spectra are speculated to be the result of field-varying electron-neutral and electron-ion collisional dynamics. In this model the electron and ion densities are assumed to be sufficiently small to allow the magnetic field to permeate the bulk of the plasma even at the highest field strengths. An estimate of the diffusion time τ for the field into the plasma at the peak density and at maximum magnetic field gives $\tau \approx 0.7 \mu\text{s}$. This time rapidly declines with decreasing magnetic field ($\tau \propto B^2$).

Larmor gyrations describe the dynamics of charged particles in magnetic fields. The Larmor radius a_L of a particle in a magnetic field B depends on its velocity component perpendicular to the direction of \mathbf{B} ,

$$a_L = \frac{v_{\perp}}{\omega_c}, \quad (4)$$

where $\omega_c = qB/mc$ is the cyclotron frequency of a particle of mass m and charge q moving in a magnetic field B . The quantity c is the speed of light. The electron and ion cyclotron frequencies at maximum magnetic field ($B = 300 \text{ G}$) are $\omega_{ce} = 5.28 \times 10^9 \text{ rad/s}$, $\omega_{ci} = 2.10 \times 10^4 \text{ rad/s}$. An estimate for the electron Larmor radius, using $v_{\perp} = 6.1 \times 10^7 \text{ cm/s}$, is $a_{Le} = 110 \mu\text{m}$. For ions, a similar estimate using $v_{\perp} = 2.4 \times 10^5 \text{ cm/s}$ gives $a_{Li} = 11.4 \text{ cm}$. This velocity choice for the ions is based on the corresponding velocity calculated from the experimental data for neutrals at $23 \mu\text{s}$ and the geometry of the ionic fluorescence. Since the ion peak occurred at an earlier time ($8 \mu\text{s}$), the ion velocity was assumed to be a factor of 3 larger than the neutral velocity.

Many interactions between particles in the plasma are possible. The high mean transverse velocity of the electrons, ensuring high numbers of electron-ion and electron-neutral collisions in the plasma, makes the electrons likely candidates for the energy exchange process.

The primary physical effect that causes the changing fluorescence is increasing confinement of the charged plasma constituents due to an increasing magnetic field. The magnetic field does not change the kinetic energy of any of the plasma constituents under collisionless conditions. However, magnetic-field confinement can indirectly change the kinetic energy of different plasma species by affecting the frequency and number of inelastic collisions. In addition, magnetic-field confinement can change the velocity distributions of the ions and electrons. Consider electrons and ions in a field-free situation. Particles with high transverse velocities and correspondingly lower longitudinal velocities strike the wall and are lost before reaching the viewing area 10 cm downstream from the source. When an axial magnetic field is applied, the electrons will have the same longitudinal speed as before but, instead of being lost, they will execute gyro orbits and collide with neutral atoms and ions. The increase in collisions due to such confinement will cause fluorescence changes.

Except at the very lowest magnetic fields, the plasma

has a very low magnetic β , i.e.,

$$\beta = \frac{n_i k T_i + n_e k T_e}{B^2 / 8\pi}, \quad (5)$$

where the numerator corresponds to the plasma pressure and the denominator is the magnetic pressure. In this expression $n_{e,i}$ are the electron (ion) densities. At the densities and temperatures in these experiments the plasma beta has the value $\beta=1$ at a magnetic field of about 2 G. Thus, for most of the magnetic-field range used in these experiments the plasma beta was less than 1.

In zero magnetic field, the electrons undergo few interactions with each other and with other particles of the plasma. The observed fluorescence at zero magnetic field is due to cascades from higher-lying levels that are still decaying 10 μ s after the laser pulse. When the magnetic field is applied, the number of electron-neutral and electron-ion interactions increases, resulting in quenching of cascade radiation from all levels (high and low) in both heavy species (atoms and ions). The quenching mechanism for excited ions is superelastic-electronic collisions. For excited neutrals two mechanisms are possible: superelastic collisions with electrons and, for higher-lying levels, electron impact ionization. The electron temperature rises due to superelastic collisions with excited neutrals and ions.

As the plasma confinement becomes more effective with increasing magnetic field, the number of electron-neutral and electron-ion interactions rises and the electrons begin returning energy to the ions and neutral atoms, since the electrons have quenched most excited states and now encounter ground-state ions and neutrals. The fluorescence from low-lying neutral and ion lines will start to increase, with the largest increase occurring in ionic fluorescence due to better overlap of the electron-ion spatial distributions and also due to higher electron-ion inelastic cross sections. This is demonstrated by the large rate of increase in the intensity of the four observed transitions from the two low-lying ionic P levels when the magnetic field rose; the corresponding lines are those at 6143, 4935, 6499, and 4555 \AA [see Figs. 3(b) and 4 and Table I]. In contrast, the radiation from transitions out of the low-lying P levels in neutral Ba, such as the 7913- and 5537- \AA lines, exhibited a much smaller rate of increase with increasing magnetic field. At the maximum magnetic field the strong 5537- \AA line of neutral barium has roughly a fifth the intensity present in any one of the low-lying ion lines. Both neutral and ionic barium have metastable D states at about 1 eV (see Fig. 3). Since the energy gap between these levels and the low-lying P levels is on the order of the mean electron energy, electronic excitation from the D to the P levels causes a rapid increase in the low-lying P level populations as the magnetic field rises.

The rising populations of low-lying excited states in the ions and neutrals cause higher-lying levels to become populated through collisions with electrons. The fluorescence from transitions out of these higher-lying levels should increase with increasing magnetic field. The rate dI/dB at which the higher-lying level fluorescence will

increase with magnetic field depends on the relative energy gap between these higher-lying levels and the low-lying levels. For example, since the high-lying ion levels, e.g., $6d^2D_{3/2}$ and $6d^2D_{5/2}$ —see Fig. 3(b), lie far above the low-lying P levels ($E_{\text{gap}} \approx 3$ eV), it is expected that the transitions associated with these higher-lying levels will increase very slowly as B is increased. This is clearly demonstrated by Fig. 5(e), which shows the I - B characteristic curve of the 3893- \AA line due to a transition out of the high-lying $6d^2D_{3/2}$ ion level. In contrast, for the neutrals the levels are more closely spaced and so the neighboring levels to the $6s6p^1P_1$ low-lying level rise in population more rapidly with increasing B than in the ion case. This can be seen from the I - B characteristic of the $5d6p^3D_3 \rightarrow 5d6s^3D_3$ line at 6500 \AA in neutral Ba—see Fig. 5(b).

As the magnetic field is further increased, the electronic excitation rate of higher-lying levels will increase, thereby removing electrons from the low-lying excited levels of the neutrals and ions. For example, in Ba^+ ions the $6p^2P_{1/2}$ level depopulation rate will increase with increasing B because ions in this level will have a higher probability for undergoing a collision with an electron that excites the ion to a higher-lying level like the $6d^2D_{3/2}$ level—see Fig. 3(b). Eventually, the production and destruction rates of the low-lying excited states will become equal and one would expect the I - B curves of some of these states to start showing saturation behavior at high- B field values. Such behavior was observed in only one case, that of the 4555- \AA line in Ba^+ . This result is expected since the highest energy low-lying level of the ion (the species most affected by electron collisions) is closest in energy to the higher-lying D levels [see Fig. 3(b)].

Finally, radiation transport is an important consideration in plasma-field interaction dynamics. In the experiments discussed in this paper, the only line that was optically thick was the Ba 5537- \AA line. Optical thickness estimates were made using the following assumptions.

(1) Level populations followed Boltzmann distributions with an ion temperature of $kT_i \approx 0.8$ eV and a neutral temperature of $kT \approx 0.36$ eV.

(2) Both ion and neutral lines were Doppler broadened to 1 GHz. All neutral and ion lines other than the 5537- \AA line in neutral Ba were calculated to be optically thin.

CONCLUSIONS

The line radiation emitted by a streaming plasma was observed to be strongly dependent on small magnetic fields. Integrated fluorescence of individual lines passed through minima, decayed, or grew rapidly as a function of increasing magnetic field. Measurements support a model in which the energy lost by the quenched higher-lying levels excites lower-lying levels using electrons as an intermediary. Further investigation is needed to verify the assumptions of the model and to provide a calculated fit of the measurements presented in this paper. Measurements of I - B curves at magnetic fields higher than 300 G would clearly define the saturation of level populations. In addition, a reliable measurement of the electron

density as a function of magnetic field would help elucidate the detailed causes of the changes in fluorescence emitted by the Ba streaming plasma.

ACKNOWLEDGMENTS

The authors are grateful for the support of the Department of Energy under Contract No. LLNL/DOE S/S

1 133 303 and the Army Research Office under Contract No. DAAL-87-K-0068. We thank Michael Kadar-Kallen for first pointing out the effect and for his technical assistance, and we thank Carl Collins for the use of his diode laser. The authors appreciate the discussions and comments by Professor Francis Perkins. Will Happer is to be thanked for a critical reading of the manuscript. One of us (T.G.M.) would like to thank the National Science Foundation for financial support.

-
- ¹T. P. Hughes, *Plasmas and Laser Light* (Hilger, London, 1975), pp. 429–435.
²David W. Koopman, *Phys. Fluids* **19**, 670 (1976).
³H. Schwarz and H. Hora, in *Laser Interactions and Related Plasma Phenomena*, edited by H. Schwarz (Plenum, New York, 1971), p. 301.
⁴G. Jellison and C. R. Parsons, *Phys. Fluids* **26**, 1171 (1983).
⁵B. H. Ripin, E. A. McLean, C. K. Manka, C. Pawley, J. A. Stamper, T. A. Peyser, A. N. Mostovych, J. Grun, A. B. Hassam, and J. Huba, *Phys. Rev. Lett.* **59**, 2299 (1987).
⁶P. Moskowitz, F. Whitney, and J. Maya, *J. Illum. Eng. Soc.* **16**, 105 (1987).
⁷J. Maya and R. Lagushenko, in *Advances in Atomic, Molecular, and Optical Physics*, edited by B. Bederson and A. Dalgarno

- (Academic, Orlando, 1990), Vol. 26, pp. 346–349.
⁸T. -M. Zhou, L. -Z. Wang, D. D. Hollister, S. M. Berman, and R. W. Richardson, *J. Illum. Eng. Soc.* **16**, 176 (1987).
⁹D. W. Koopman, *Phys. Fluids* **14**, 1707 (1971); S. S. Segall and D. W. Koopman, *ibid.* **16**, 1149 (1973).
¹⁰R. J. von Gutfeld and R. W. Dreyfus, *Appl. Phys. Lett.* **54**, 1212 (1989).
¹¹J. G. Laframboise and J. Rubinstein, *Phys. Fluids* **19**, 1900 (1976); J. Rubinstein and J. G. Laframboise, *ibid.* **26**, 3624 (1983).
¹²E. P. Szuszcwicz and P. Z. Takacs, *Phys. Fluids* **22**, 2424 (1979).
¹³G. P. Jellison, Ph.D. thesis, University of Maryland, 1981; G. Jellison and C. R. Parsons, *Phys. Fluids* **24**, 1787 (1981).

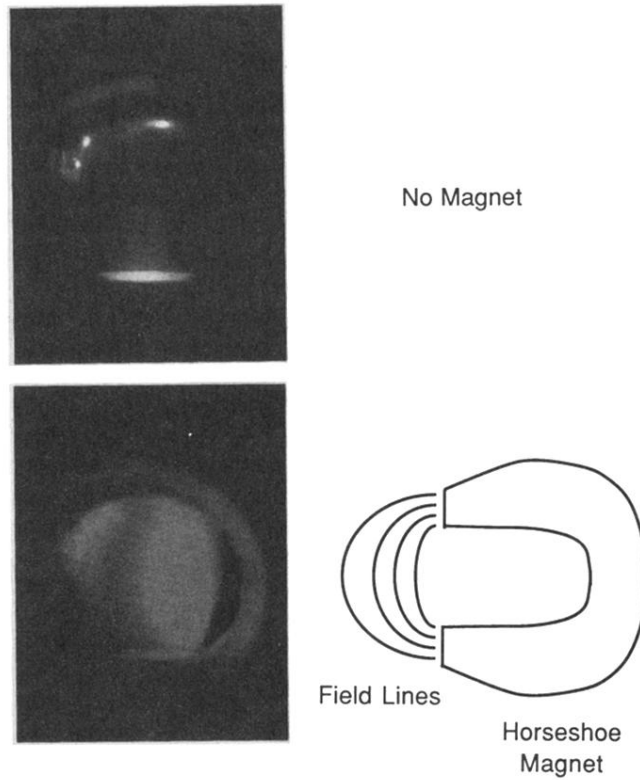


FIG. 1. Images taken with a CCD camera reveal the spatial variations of fluorescence in the central region of the chamber when (a) no magnetic field was applied and (b) when a 1-kG horseshoe magnet was placed next to the chamber as indicated. The laser-produced plasma flows up in these images. The viewing region is 10 cm from the barium target. The spatial distribution of the enhanced fluorescence shows that the radiation is highly localized.